

## HIGH-RESOLUTION REFLECTIVITY INVERSION

THANG NGUYEN and JOHN CASTAGNA

*Department of Earth and Atmospheric Sciences, The University of Houston, 4800 Calhoun Rd., Houston, TX 77204, U.S.A. 3dseismic@sbcglobal.net*

(Received April 9, 2010; accepted June 26, 2010)

### ABSTRACT

Nguyen, T. and Castagna, J., 2010. High-resolution reflectivity inversion. *Journal of Seismic Exploration*, 19: 303-320.

Assuming the convolutional model and a known wavelet, reflectivity inversion is an ill-posed problem. Existing methods mostly regularize the problem using mathematical criterion, such as minimization of the reflectivity vector norm. We propose reflectivity inversion using atomic decomposition, in which the atoms can be basic geological structures or derived from well logs. This is equivalent to replacing mathematical criterion by geological ones. Numerical results show that atomic decomposition is robust to noise. When applied to multi-dimensional data in a trace by trace basis, atomic decomposition shows lateral instability. The solutions are non-unique. Atomic decomposition results are probable solutions, which can be laterally regularized by re-projection.

**KEYWORDS:** reflectivity, inversion, matching pursuit, regularization, geological pattern, sparse spike inversion, basis pursuit.

### INTRODUCTION

Seismic images provide very useful subsurface geological information. The seismic image in time is a collection of wiggle traces at surface locations. The fundamental problem is that these traces always bear the source signature wavelet, which smears adjacent events and reduces the resolution of the image. In general, hydrocarbon reservoirs are thinner than the length of the wavelet. Therefore, increasing the resolution of the seismograms is of utmost importance for imaging thin layering.

Tremendous amount of work has been done since the birth of the digital computers in order to improve the seismogram's resolution. Assuming the convolutional model, the seismograph is the reflectivity series convolving with the wavelet. Deconvolution seeks to remove the wavelet by an inverse filter. In the 1960's, purely statistical, or blind deconvolution, based on Wiener theory, was used (Robinson, 1957; Treitel and Robinson, 1977). These deconvolution filters were derived directly from the seismic data with statistical assumptions about the spectrum of the reflectivity and the phase of the wavelet.

In the 1970's, deterministic deconvolution, which assumes that the wavelet is known *a priori*, was developed. We cast deterministic deconvolution as an inverse problem. Inversion of seismic reflectivity is understood in a generalized sense as increasing resolution or enhancing frequency content. In the ideal case, the true seismic reflectivity is recovered. In reality, the goal is to achieve the best results using both objective and subjective criteria.

Most deterministic deconvolution methods use an optimization algorithm to find the reflectivity. Optimization methods differ in the cost functional, the regularization functional, and the descending algorithm. The cost functionals are usually some measure of energy of the misfit. Because the wavelet is always band-limited, the matrix representing the convolution operator is highly degenerate. The linear inverse problem is ill-posed, and requires regularization to achieve stable results. The regularization functional takes the form of the  $L_p$ -norm of the reflectivity vector. Descent algorithms are usually gradient-based (Santosa and Symes, 1986) or linear programming (Taylor et al., 1979; Oldenburg et al., 1983). Taylor et al. (1979) used the  $L_1$ -norm of the solution as a regularization functional, resulting in a spiky reflectivity. Debeye and Riel (1990) expanded this method and used the  $L_n$ -norm of the solution as a regularization functional. Regularization with the  $L_1$ -norm is called sparse-spike inversion (SSI). This is a very popular method and has been implemented utilizing different algorithms (Levy and Fullagar, 1981; Oldenburg et al., 1983; Kim et al., 2007). In this paper, our results will be benchmarked against SSI.

The central idea in inverse theory is the prescription (Press et al., 1992)

$$\text{minimize: } A + \lambda B \quad , \quad (1)$$

where  $A$  is a functional measuring the agreement of the model with the data, and  $B$  is a regularization functional. Inversion methods differ in the choice of  $A$  and  $B$ . This prescription also underlines the compromise between inversion sharpness and stability.

Sparse-spike inversion utilizes the  $L_2$ -norm of the misfit for  $A$ , and the  $L_1$ -norm of the model vector for  $B$ . Minimization the  $L_1$ -norm of the model vector

results in spiky reflectivity. This is ingenious because 1) linear inverse theory proves that  $L_1$ -norm regularization operator stabilizes the inversion and 2) sparse-spike reflectivity is desirable. Donoho (2004) proved that the  $L_1$ -norm solution is the sparsest solution. Dossal and Mallat (2005) gave analytical formula to estimate resolving power of  $L_1$ -norm deconvolution. Daubechies et al. (2004) proved that using  $L_p$ -norm of the vector as regularizing penalty does regularize the problem, for  $1 \leq p \leq 2$ .

However, the  $L_1$ -norm could be considered merely mathematical convenience. While at times, the real reflectivities do agree with the minimization of some mathematical quantity, one does not have explicit control over the process. Minimizing the  $L_1$ -norm corresponds to a spiky reflectivity; yet why the earth's reflectivity cares about its spikiness? We know that some fundamental geological structures, such as ramps, are not spiky. One can only hope, at best, that spikier reflectivities more resembles the real earth. We fully appreciate the ingenuity of this stabilization functional; however one must admit that it is very hard to relate sparsity to geology.

Our approach is geological. It provides a systematic way to incorporate all a priori knowledge into the inversion process. It also allows incorporating guesses, therefore tailoring the inversion results. The idea is that in a vicinity, the same geological structures tend to repeat at different scales and locations. Another word, the earth's reflectivity is not some random series; instead, there are some geological structures (or models) that are most frequently encountered. Furthermore, the unknown reflectivity in a partly explored area can be expected to contain structures similar to known reflectivities nearby.

The inversion is carried out using an atomic decomposition method, in particular matching pursuit (MP) (Mallat and Zhang, 1993). The method is a nonlinear, greedy, adaptive approximation that successively decomposes a signal into a sum of atoms chosen from a dictionary. It is greedy in the sense that when a particular atom is chosen, its maximum contribution is used. A dictionary is a redundant set of atoms designed to best represent and capture the main features of a signal. In our application, an atom is a convolution of the known wavelet and a possible reflectivity.

Numerical examples show that while being robust to random noise, matching pursuit based inversion is not stable. The results only reflect one solution out of an infinite number of probable solutions. We propose to re-project the data into an interpretive basis to stabilize the solution.

The idea of using matching pursuit decomposition incorporating signal-matched dictionaries has been implemented elsewhere (for example Papandreou-Suppappola and Suppappola, 2002). Herrmann (2005) tackled the blind deconvolution problem using smooth wavelet with vanishing moments and

a dictionary of fractional splines for reflectivity. Herrmann compared results using two different atomic representations: matching pursuit and basis pursuit (Chen et al., 2001). Unlike MP, which greedily projects the residue at each iteration to the best matched atom, basis pursuit (BP) solves for all atom coefficients at once using a global optimization for sparsity. Atomic deconvolution results in Herrmann (2005) showed that both methods suffered from instability. BP tends to resolve better than MP when the dictionary is simple, but fails when the dictionary becomes extensive.

Our model-matching approach is related to spectral inversion (Partyka et al., 1999; Partyka, 2001, 2005). High-resolution reflectivity inversion results have been achieved (Portniaguine and Castagna, 2005; Chopra et al., 2006, 2007) when the spectra are computed using sparse inversion (Portniaguine and Castagna, 2004).

## METHODS

We present the basic equations of matching pursuit. Details can be found in Mallat and Zhang (1993); Mallat (1998). MP is a nonlinear adaptive approximation which decomposes a signal into a weighted sum of chosen atoms taken from a dictionary. The dictionary is designed such that its atoms contain dominant features of the signal, and the result of the decomposition is readily interpretable.

Let  $D = \{g_{\gamma} \in \mathcal{R}\}$  be a unit norm dictionary. A matching pursuit begins by projecting  $f$  over a vector  $g_{\gamma_0} \in D$  and computing the residue  $Rf$ :

$$f = \langle f, g_{\gamma_0} \rangle g_{\gamma_0} + Rf, \quad (2)$$

$Rf$  is orthogonormal to  $g_{\gamma_0}$ . Indeed,

$$\langle Rf, g_{\gamma_0} \rangle = \langle f - \langle f, g_{\gamma_0} \rangle g_{\gamma_0}, g_{\gamma_0} \rangle = 0.$$

Therefore, energy is conserved

$$\|f\|^2 = |\langle f, g_{\gamma_0} \rangle|^2 + \|Rf\|^2, \quad (3)$$

To minimize  $\|Rf\|$  we must choose  $g_{\gamma_0}$  such that  $|\langle f, g_{\gamma_0} \rangle|$  is maximum ( $g_{\gamma_0}$  has the highest correlation to the signal).

The pursuit iterates this procedure by subdecomposing the residue. Let  $R_0 f = f$ . Suppose that the  $m$ -th order residue  $R^m f$  is already computed, for  $m \geq 0$ . The next iteration chooses  $g_{\gamma_m} \in D$  such that  $|\langle R^m f, g_{\gamma_m} \rangle|$  is maximum. Project  $R^m f$  on  $g_{\gamma_m}$ ,

$$\mathbf{R}^m \mathbf{f} = \langle \mathbf{R}^m \mathbf{f}, \mathbf{g}_{\gamma_m} \rangle \mathbf{g}_{\gamma_m} + \mathbf{R}^{m+1} \mathbf{f} . \quad (4)$$

The orthogonality of  $\mathbf{R}^{m+1} \mathbf{f}$  and  $\mathbf{g}_{\gamma_m}$  implies

$$\|\mathbf{R}^m \mathbf{f}\|^2 = |\langle \mathbf{R}^m \mathbf{f}, \mathbf{g}_{\gamma_m} \rangle|^2 + \|\mathbf{R}^{m+1} \mathbf{f}\|^2 . \quad (5)$$

Summing eq. (4) from  $m$  between 0 and  $M - 1$  gives

$$\|\mathbf{f}\|^2 = \sum_{m=0}^{M-1} |\langle \mathbf{R}^m \mathbf{f}, \mathbf{g}_{\gamma_m} \rangle|^2 + \|\mathbf{R}^M \mathbf{f}\|^2 . \quad (6)$$

Eq. (6) depicts a very important feature of matching pursuit: energy is conserved just as in an orthogonal decomposition. When the dictionary  $D$  completes the signal space, the residual  $\|\mathbf{R}^m \mathbf{f}\|$  converges exponentially to 0 when  $m$  tends to infinity. Notice that even though  $\mathbf{f}$  is of finite dimension, it takes an infinite number of iterations to completely zero the residue. In seismic processing, this is not an issue because the number of atoms needed to capture dominant features of the signal is usually much less than the number of samples.

For our application, the dictionary is a set of atoms  $\psi_{\gamma_w}(t - t_0)$ , which are convolutions of seismic wavelet  $w(t)$  and geologically feasible patterns  $\psi_{\gamma}(t - t_0)$ . The pattern  $\psi_{\gamma}(t - t_0)$  is defined by its index  $\gamma$ , which includes its type and scale, and is centered at  $t_0$ . This dictionary satisfies the translation-invariant condition:

$$\forall \mathbf{g}_{\gamma} \in D \text{ and } p \in [0; N-1] \text{ then } \mathbf{g}_{\gamma}[n - p] \in D . \quad (7)$$

Dictionary patterns can be basic geological structures, such as layers, ramps, thin beds, or features derived from well logs. Layers tend to have sharp transitions, whereas ramps are more gradual. They are modeled as step functions, with different degrees of smoothing. Thin beds are frequently encountered; therefore they should have their own type. Thin bed thickness is limited to the length of the wavelet; thicker beds can be represented by two step functions. Fig. 1 shows examples of layers, ramps and thin beds.

Overlapped structures can be extracted from a well log. The extraction can be done manually, or automatically. For example, one algorithm we used to extract these features locates local extrema in the impedance log, then forms features between adjacent extrema and between every other extrema. Once extracted, the structures are scaled to different lengths using spline interpolation. For example, Fig. 2 shows 12 impedance features extracted from a real well log. The log has been converted to time and resampled to reflect a 4 ms sampling in the seismic.

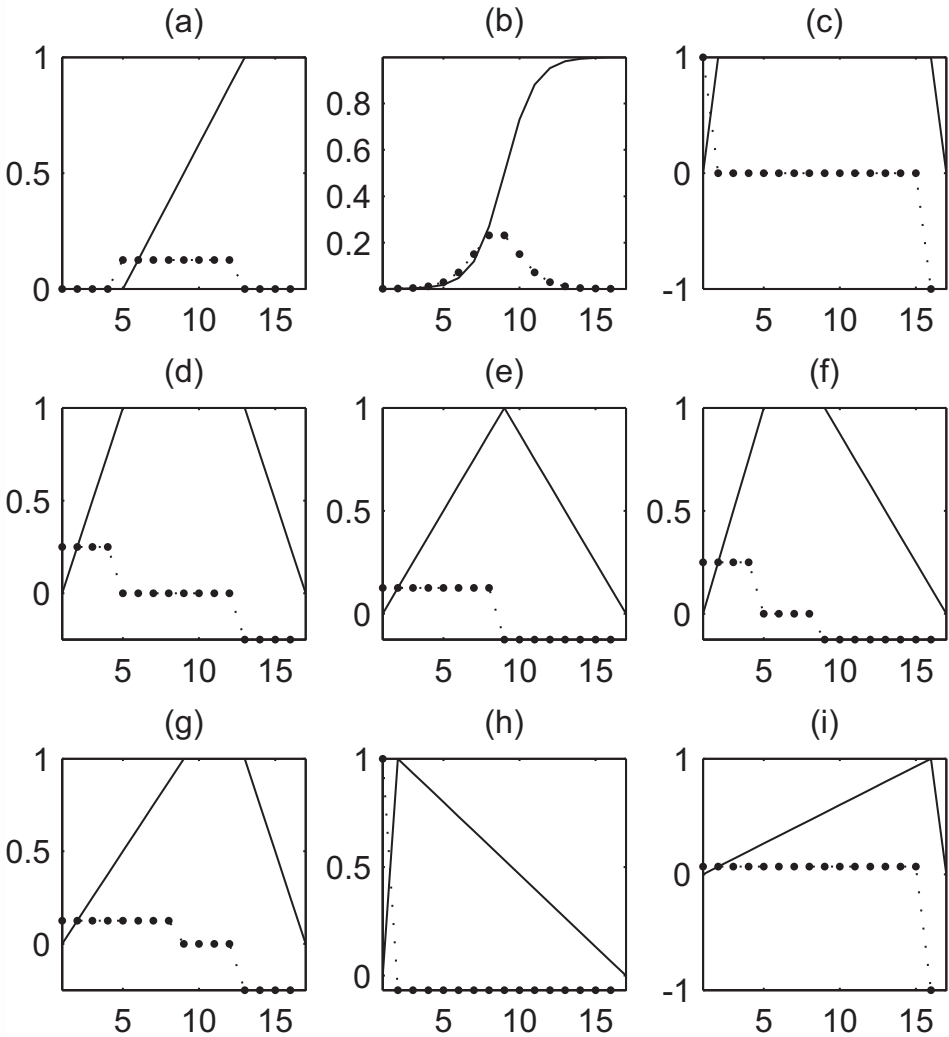


Fig. 1. Basic geological structures. Solid lines are impedances, dotted lines are reflectivities. These fundamental structures are scaled to form the dictionary. (a) and (b) show example of layer structures, (c) to (i) illustrate a variety of thin beds.

In many situations, we need to bias the matching-pursuit selection. For example, when inverting with geological structures derived from well logs, distance between the well and the inverting trace (proximity) is taken into consideration. Atoms derived from closer well are more favorable than those derived from father wells. The ability to bias the cross-correlation before searching for the best-matched atom makes matching pursuit very flexible.



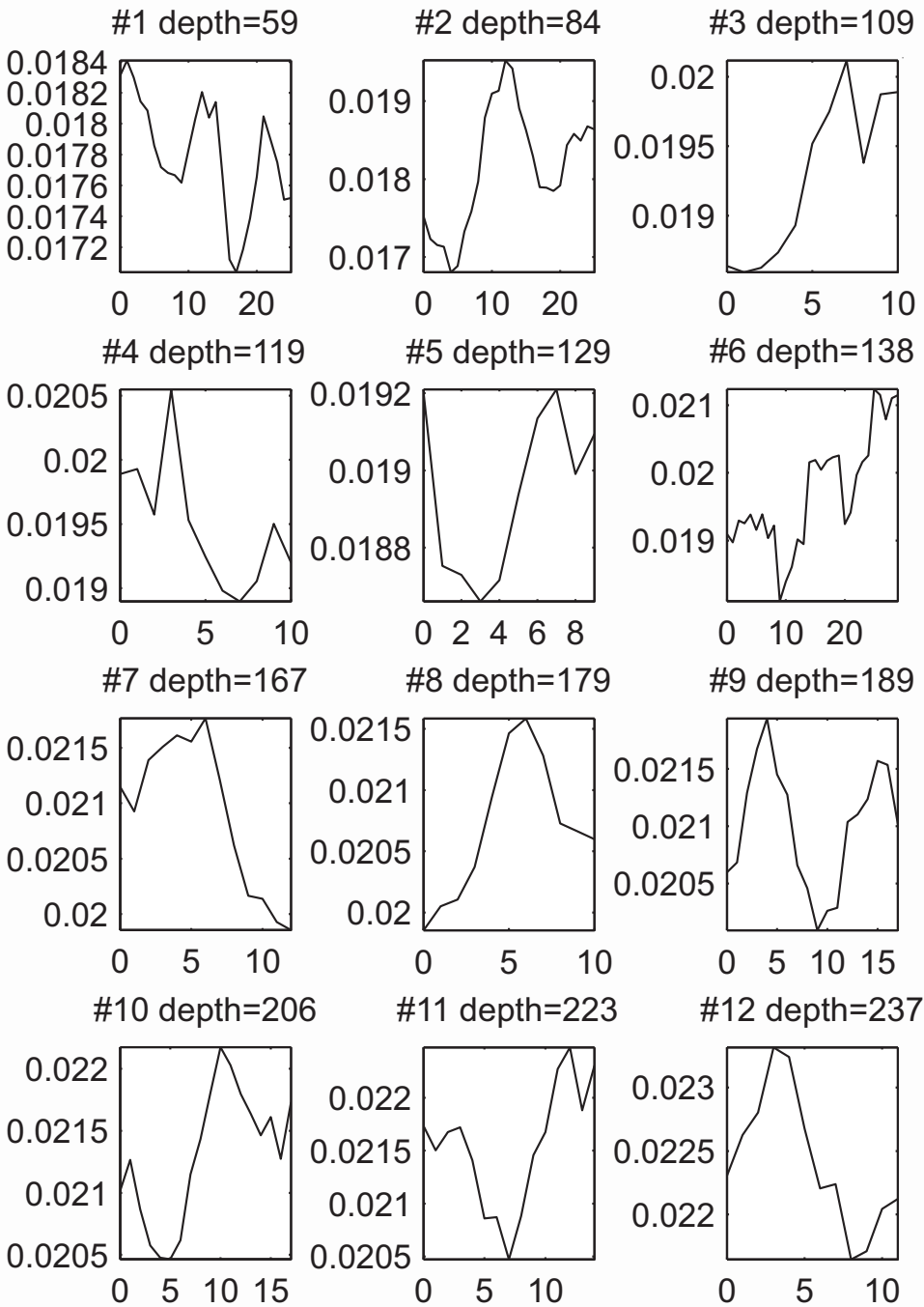


Fig. 2. Derived features from a real well log. Only 12 impedance structures are shown. The unit for the x-axis is sample, which is 4 ms.

Straightforward implementation of MP-based inversion (MPI) produces unstable results, which are exemplified when applied to a laterally slow-varying gather. This sensitivity is also reported in Herrmann (2005). The problem is that we only have a limited number of patterns in our dictionary. The discontinuity from one pattern to another is significant. From one trace to the next one, when the data changes a little bit, the algorithm can pick a different atom, resulting in a quite different reflectivity. This sensitivity is common to any atomic decomposition scheme. Sparse-spike inversion does not suffer this sensitivity problem because it operates on only one type of atoms: the spikes. All parameters about the spikes: quantity, amplitude and location vary continuously. In Nguyen (2008), we proposed different methods to remedy the sensitivity problem, including (i) building slowly-varying dictionary, and (ii) constraining the atom-selection process. These methods helped, but did not solve the instability problem.

Due to the non-uniqueness nature of the problem, MPI cannot be certain about the results it produces. Switching back and forth among solutions is just a manifest of the fact that many solutions equally satisfy the convolutional model with a band-limited wavelet. The trace-by-trace inversion program only gives us an instance of all possible solutions.

For practical purpose, we propose a method, called re-projection, to stabilize the results. First, a map is formed by listing all the atoms chosen for the whole gather, descendingly sorted by correlation. Interpretation is done in the map to include/exclude atoms, change their order, or combine similar atoms. The modified map is called an interpretative basis. Second, data are projected, trace by trace, to this basis, in a manner similar to matching pursuit.

## RESULTS

It is well known that atomic decomposition are robust to random noise (Chen et al., 2001). We are more concerned about trace-by-trace stability when applying a 1D algorithm to a 2D or 3D seismic sections. A synthetic data set is created to test MPI resolving power and stability. Its geology changes gradually from one structure at one end to an entirely different one at the other end. We created such an unreal geological model by linearly interpolating the impedances from two unrelated well logs. Fig. 3 shows the reflectivity calculated from the impedance model and the synthetic data. Seismic wavelet is a 21 Hz Ricker.

Fig. 4 illustrates MP-based inversion results when no a priori information other than the wavelet is known (a), and when 6 well logs equally spaced throughout the section are known (b). The high frequency reflectivities at 2750 ms on the left most traces are difficult to recover, even with 6 well logs.



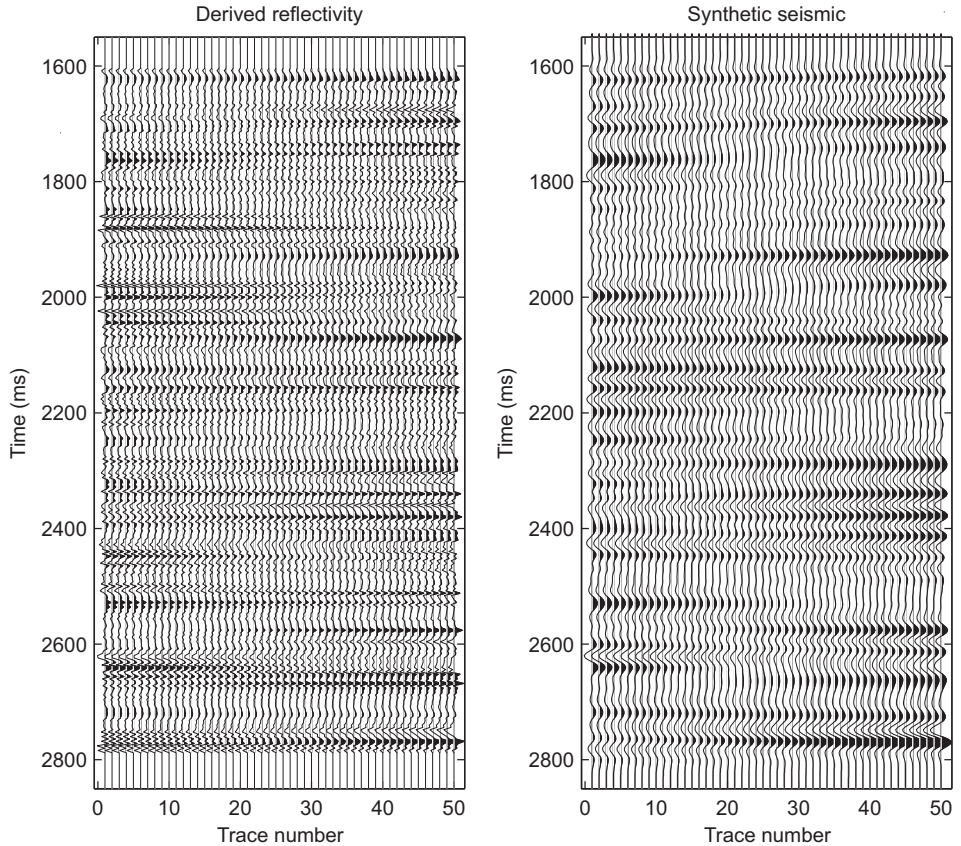


Fig. 3. Synthetic data set. (a) Reflectivity, derived from linearly interpolated impedance model. (b) Synthetic data, convolution of reflectivity and 21 Hz Ricker wavelet.

Compared to SSI results which are plotted in Fig. 5b, MPI exhibits more resolving power. As we expected, MPI results show trace-by-trace instability, especially when no logs are used. Having the logs, as in Fig. 4b depicts, helps resolve more details and reduce instability.

The results of re-projection, as discussed in the previous section, are plotted in Fig. 5a. Because the data are projected over a slowly-varying basis, the results no longer exhibit a trace-by-trace instability. Fig. 5b shows SSI results. The sparse-spike inversion program we used was developed by Kim et al. (2007).

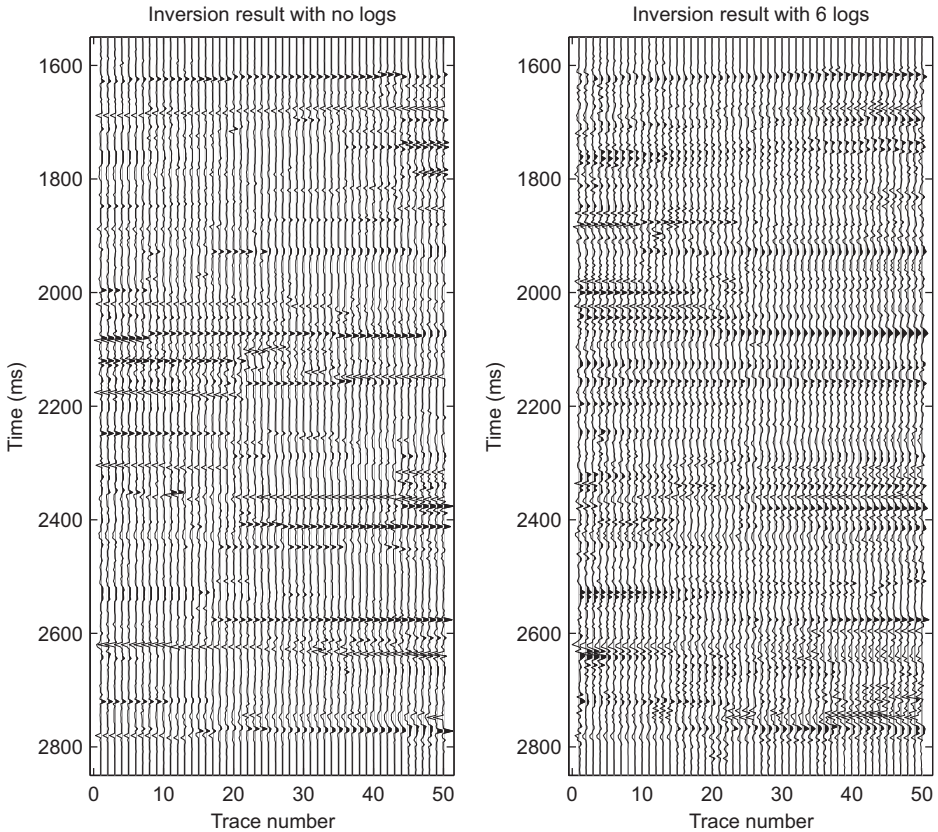


Fig. 4. MP-based inversion results. (a) Results when only the wavelet is known (b) Results when the wavelet and 6 well logs are known.

The advantage of using synthetic test is that we can quantitatively compare the goodness-of-inversion by correlating the inversion results with the known answers. Fig. 6 plots the normalized correlations of inversion results with the known reflectivity, trace by trace. Based on this resemblance, which is not necessarily the ultimate judge, MPI outperforms SSI. Re-projection compromises correlation for stability. Also, a priori information, such as well logs, significantly improves correlations.

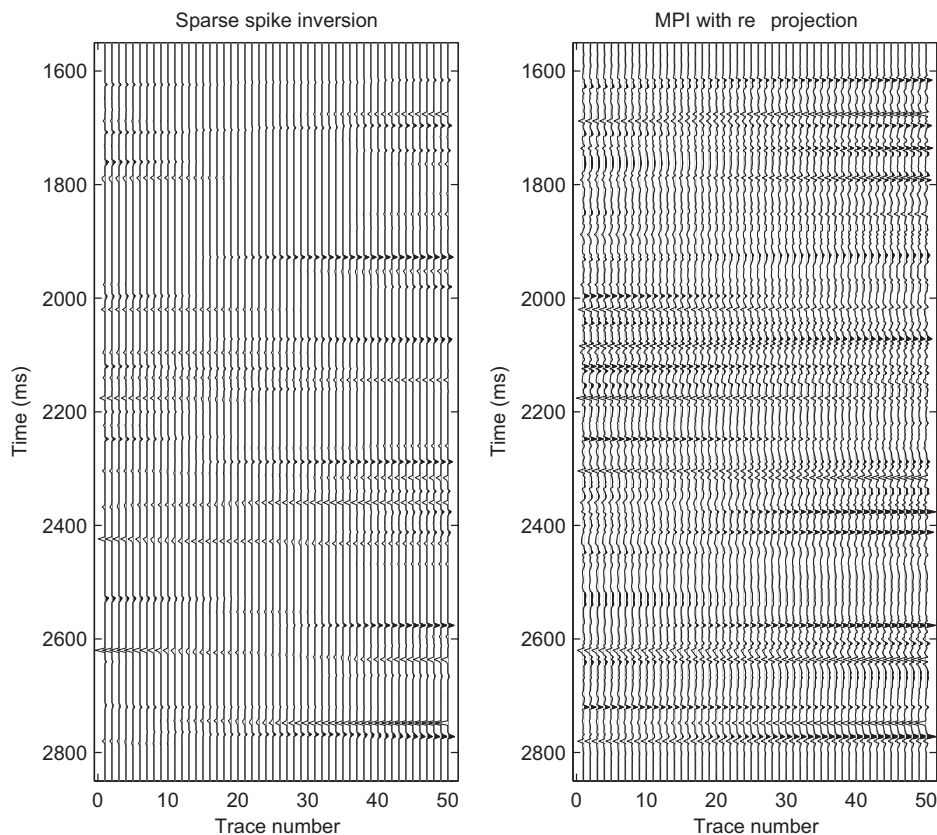


Fig. 5. Comparing MPI and SSI. (a) MPI result with no well logs used and stabilized by re-projection. (b) SSI result.

A 3D seismic dataset from South Timbalier (Louisiana, USA), along with some well logs have been made available to our research group for academic study. Details about the dataset are documented in Puryear (2006). We run the MPI over a small window where we have 78% synthetic match. The window consists of 128 traces, each trace has 1000 samples covering a time range from 1300 to 2300 millisecond. There is one well with acoustic impedance log, located at trace number 72. The top and bottom 50 ms of the window are

tapered off by a linear function to avoid edge artifacts. Fig. 7 shows the data window. Fig. 8 plots MPI results with the impedance log and stabilized using re-projection. For illustration purpose that re-projection stabilizes inversion results, we do not apply any interpretative processing to the resulting map. Fig. 9 shows SSI results as benchmarks. Fig. 10 plots detailed reflectivity traces at the well location.

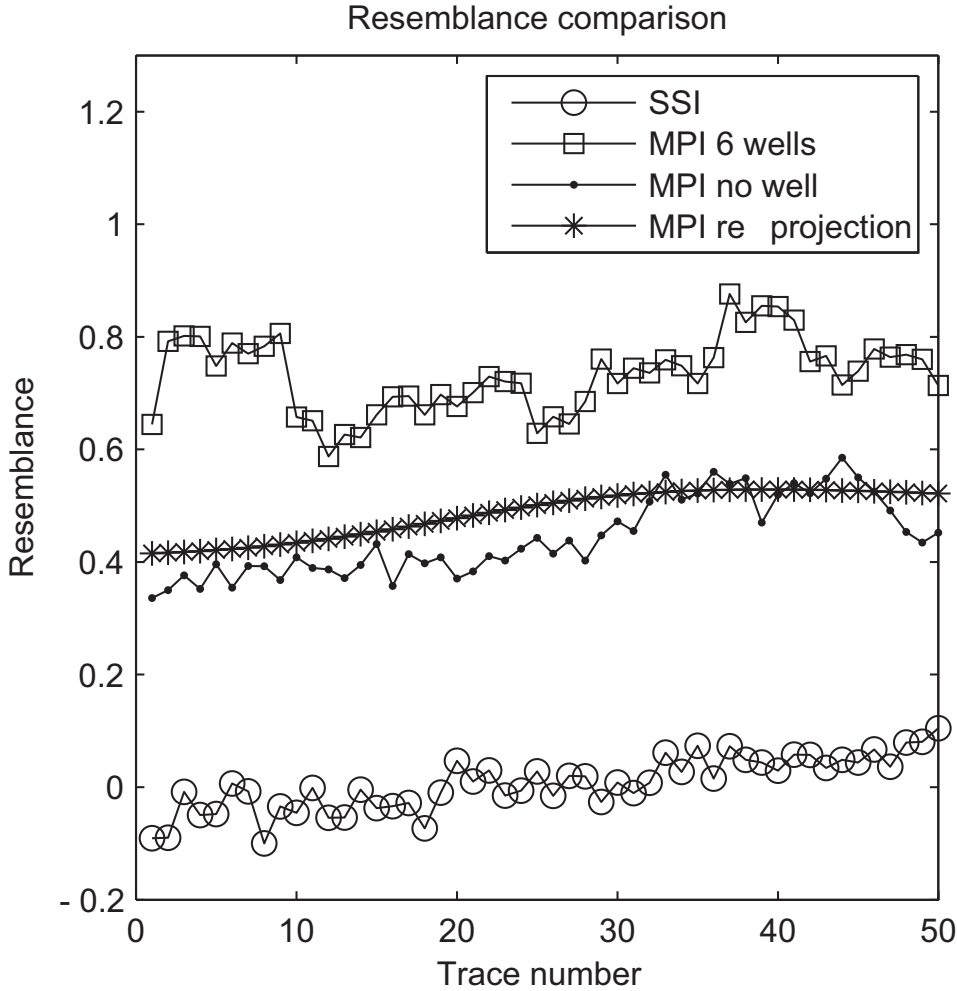


Fig. 6. Resemblance comparison of different inversions. Resemblance is normalized correlation between the inversion results and the known reflectivity.

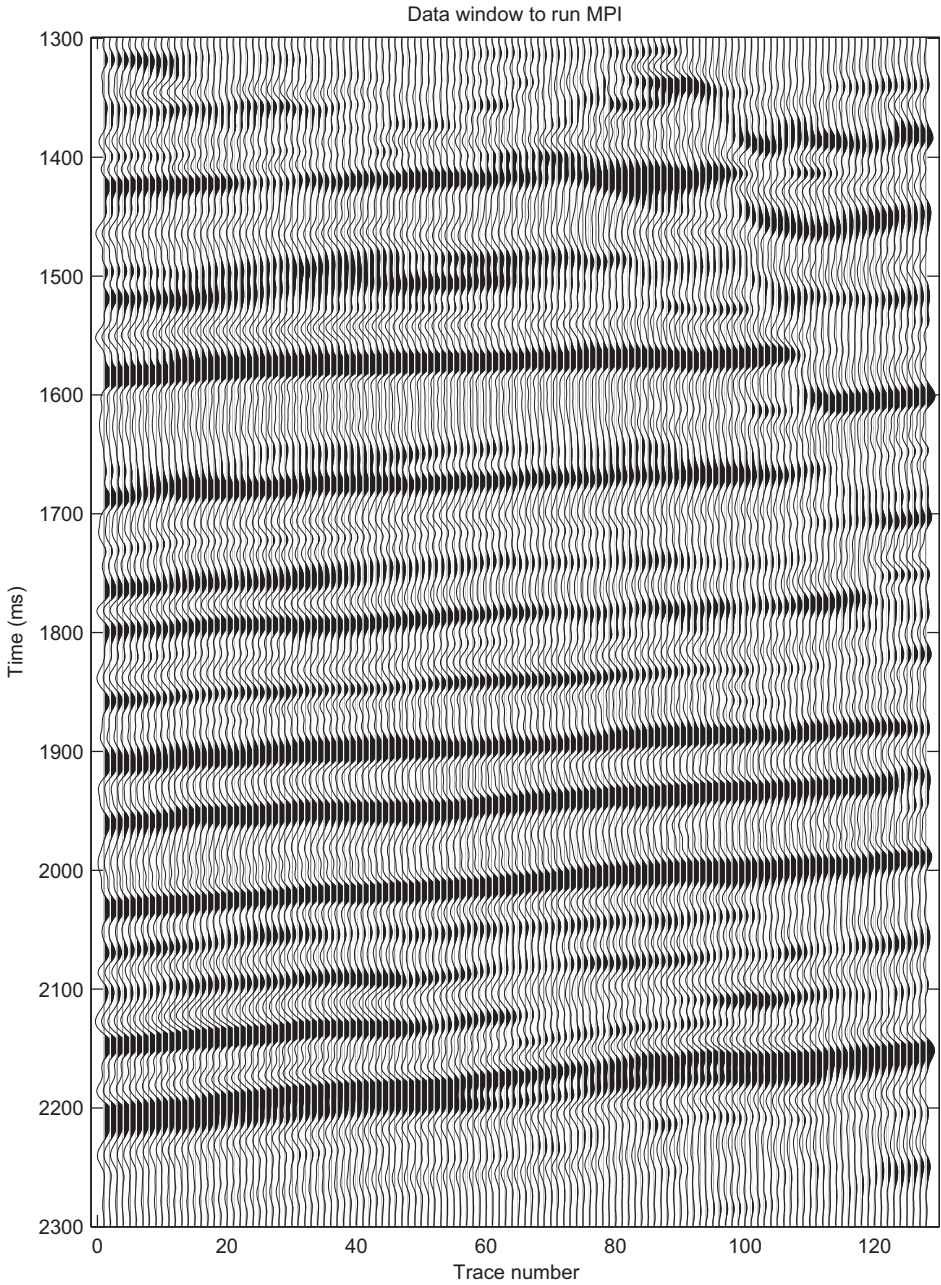


Fig. 7. Data window to run MPI. An impedance log is available at trace number 72.



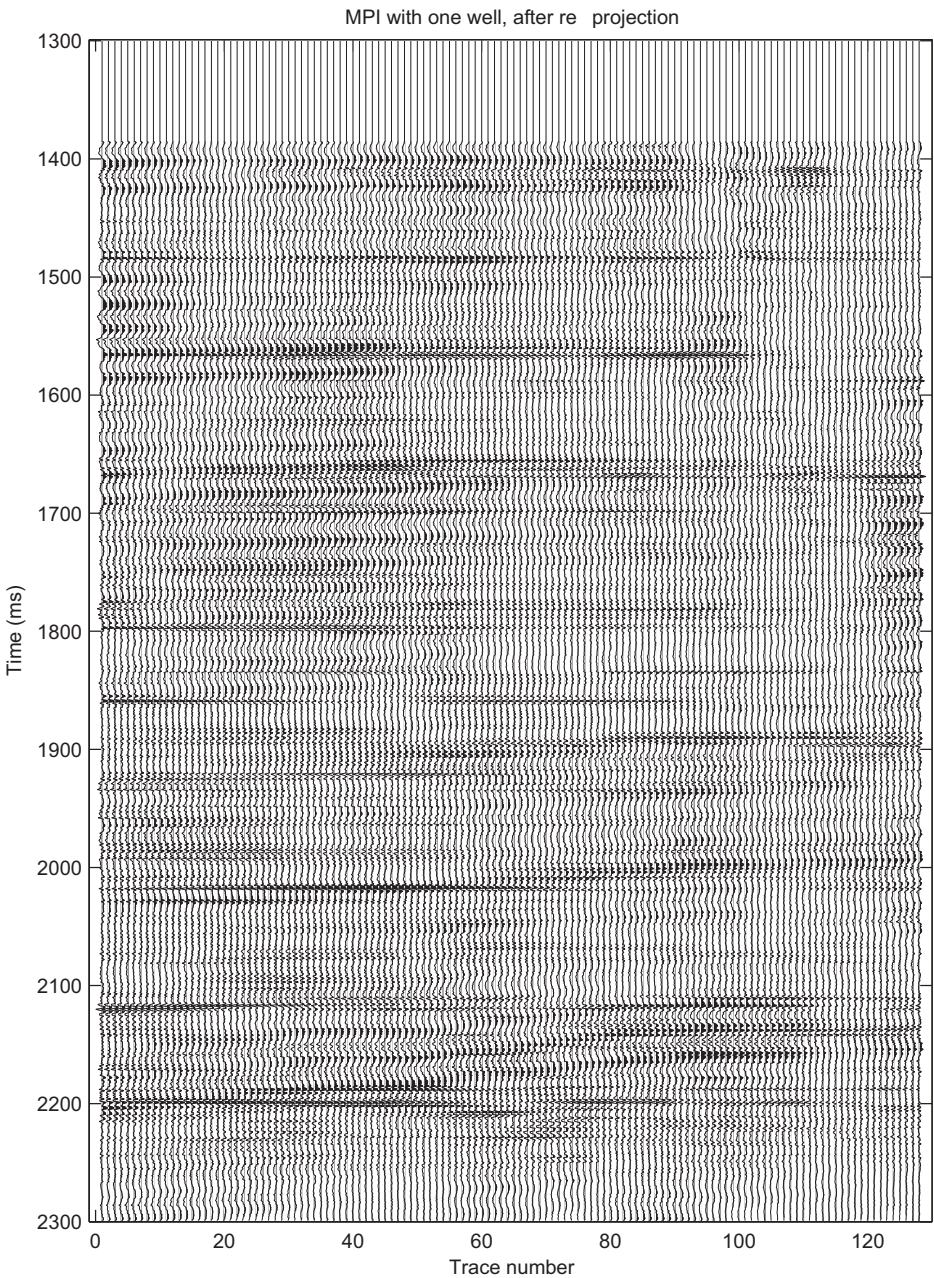


Fig. 8. MPI results after simple re-projection.



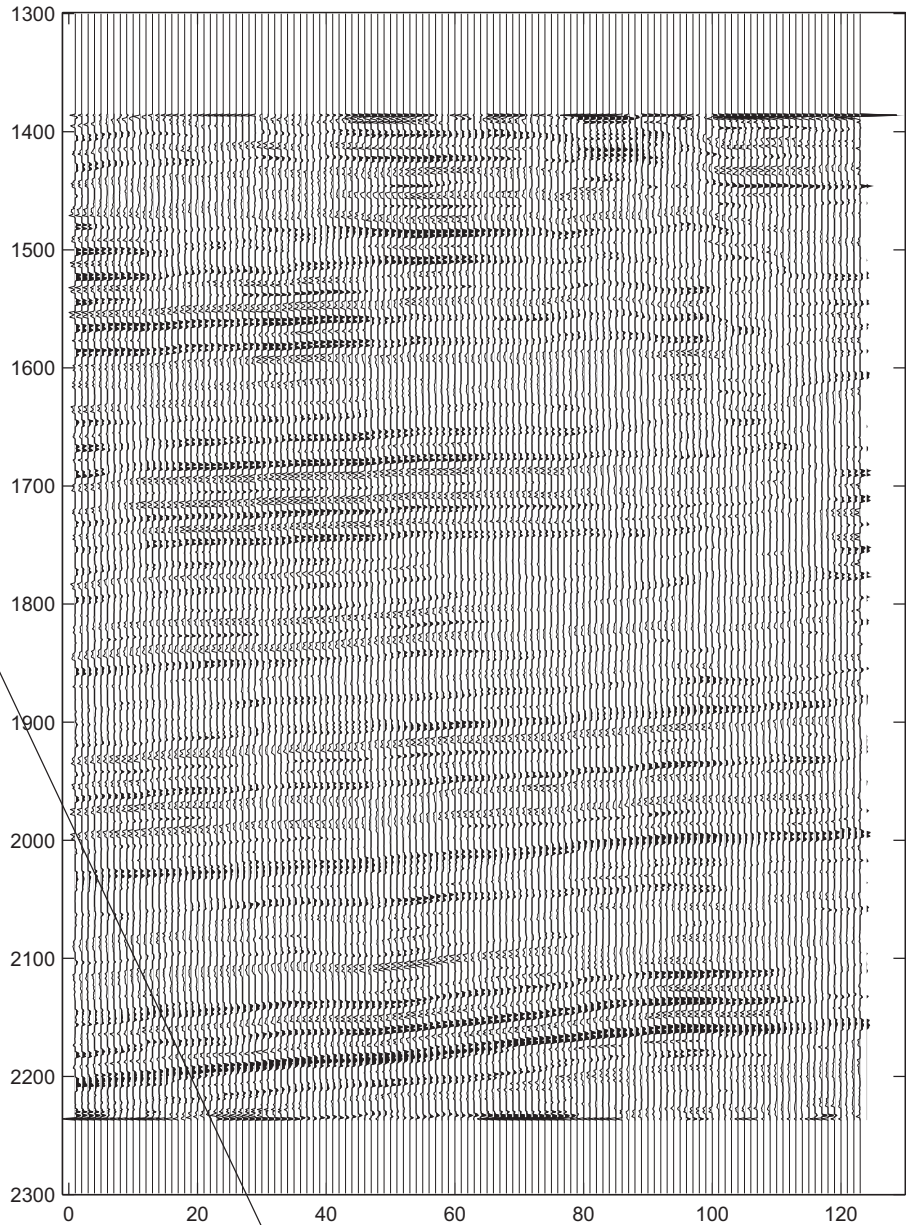


Fig. 9. SSI results. Algorithm implemented by Kim et al. (2007).

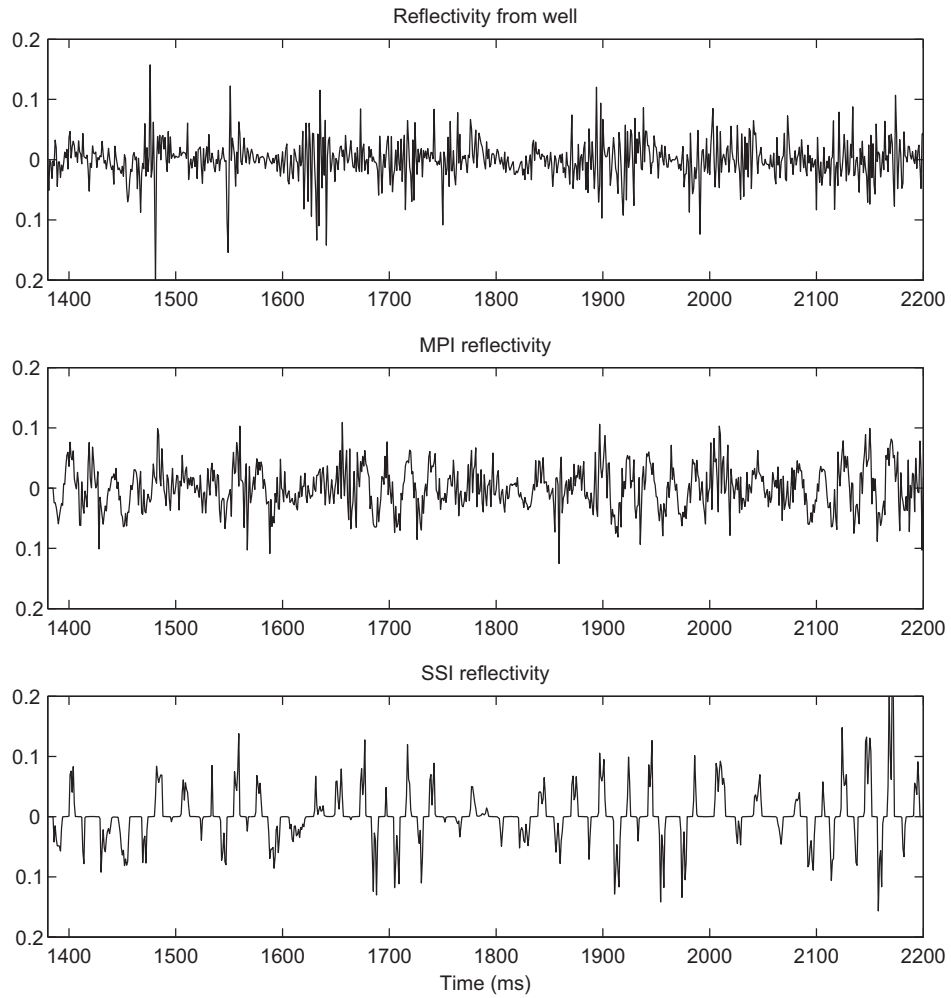


Fig. 10. Detailed reflectivities at well location.

## DISCUSSION

We feel that atomic decomposition using impulse responses of the physical system (i.e., Green's functions) is going to have many applications. Despite tremendous recent efforts on applying orthogonal wavelet theory to seismic data processing and interpretation, we think that wavelet-based seismic applications

have not delivered. Our view is that wavelet theory in general provide a dual-domain way to mathematically analyze the signals, but gives little insight to the physics of the problem. Atomic decomposition has the ability to marry the physics and mathematics aspects of the problem. The physics is involved when the dictionary is built from the Green's functions, or signatures of the system. The decomposition itself offers the analysis of the presence of each signature.

Matching pursuit has been blamed for its myopic behavior (Chen et al., 2001), leading to erroneous results and decreasing resolution. An alternative to MP-based inversion is basis-pursuit based inversion, which faces the same trace-by-trace instability. Theoretically, BP can achieve higher resolution than MP; however, in practice, one often needs to regularize his results and sacrifice resolution. Nevertheless, BP-based inversion with geological dictionary is on the top of our list for future research.

The algorithm we propose is one-dimensional. It has drawbacks when trying to apply directly to a multi-dimensional data set. The dictionary items are Green's functions for 1D earth. A multi-dimensional algorithm could be constructed using Green's function for multi-dimensional model.

Curvelets (see Candes et al. (2006) for latest curvelet mathematical development) could be used to extend sparse-spike inversion to multi-dimensions. The focus of this paper has been about wavelets in the forms of Green's functions. Perhaps after curvelet-based inversion is as popular as sparse-spike inversion now, one would have enough insight about the multi-dimensional inversion and develop appropriate physical wavelet for inversion process.

## CONCLUSION

We propose a flexible inversion method based on matching pursuit decomposition. The method allows incorporating all a priori information, as well as guesses or biases, to the inversion. Synthetic data test on real well logs show that MPI results are more accurate than sparse-spike inversion. Re-projection is needed after decomposition to regularize trace-by-trace instability. Re-projection sacrifices accuracy for stability, conforming to inverse theory.

## REFERENCES

- Candes, E.J., Demanet, L., Donoho, D.L. and Ying, L., 2006. Fast discrete curvelet transforms. *SIAM Mult. Model. Sim.*, 5: 861-899.
- Chen, S., Donoho, D. and Saunders, M., 2001. Atomic decomposition by basis pursuit. *SIAM J. Scientif. Comput.*, 43: 129-159.

- Chopra, S., Castagna, J., Xu, Y. and Tonn, R., 2007. Thin-bed reflectivity inversion and seismic interpretation. Expanded Abstr., 77th Ann. Internat. SEG Mtg., San Antonio, 26: 1923-1927.
- Chopra, S., Castagna, J.P. and Portniaguine, O., 2006. Seismic resolution and thin-bed reflectivity inversion. CSEG Recorder, 31: 19-25.
- Daubechies, I., Defrise, M. and Mol, C.D., 2004. An iterative thresholding algorithm for linear inverse problems with a sparsity constraint. *Communic. Pure Appl. Mathem.*, 57: 1413-1457.
- Debeye, H.W.J. and Riel, P.V., 1990.  $l_p$ -norm deconvolution. *Geophys. Prosp.*, 38: 381-403.
- Donoho, D., 2004. For most large underdetermined systems of linear equations, the minimal  $l_1$ -norm solution approximates the sparsest near-solution. *Communic. Pure Appl. Mathem.*, 59: 797-829.
- Dossal, C. and Mallat, S., 2005. Sparse spike deconvolution with minimum scale. *Signal Proc. Adapt. Sparse Struct. Respresent.* 123-126.
- Herrmann, F., 2005. Seismic deconvolution by atomic decomposition: a parametric approach with sparseness constraints. *Integr. Computer-Aided Engin.*, 12: 69.
- Kim, S.-J., Koh, K. Lustig, M., Boyd, S. and Gorinevsky, D., 2007. An interior-point method for large-scale  $l_1$ -regularized least squares. *IEEE J. Selected Topics Signal Proc.*, 1: 606-617.
- Levy, S. and Fullagar, P.K., 1981. Reconstruction of a sparse spike train from a portion of its spectrum and application to high-resolution deconvolution. *Geophysics*, 46: 1235-1243.
- Mallat, S., 1998. *A Wavelet Tour of Signal Processing*. Academic Press, New York.
- Mallat, S. and Zhang, Z., 1993. Matching pursuit with time-frequency dictionary. *IEEE Trans. Sign. Proc.*, 41: 3397-3415.
- Nguyen, T., 2008. High-resolution Reflectivity Inversion. Ph.D. thesis, University of Houston.
- Oldenburg, D.W., Scheuer, T. and Levy, S., 1983. Recovery of the acoustic impedance from reflection seismograms. *Geophysics*, 48: 1318-1337.
- Papandreou-Suppappola, A. and Suppappola, S.B., 2002. Analysis and classification of time-varying signals with multiple time-frequency structures. *IEEE Sign. Proc. Lett.*, 9: 92-95.
- Partyka, G.A., 2001. Seismic thickness estimation: Three approaches, pros and cons. Expanded Abstr., 71st Ann. Internat. SEG Mtg., San Antonio, 20: 503-506.
- Partyka, G.A., 2005. Spectral Decomposition. SEG Distinguished Lecture.
- Partyka, G.A., Gridley, J.A. and Lopez, J.A., 1999. Interpretational aspects of spectral decomposition in reservoir characterization. *The Leading Edge*, 18: 353-360.
- Portniaguine, O. and Castagna, J.P., 2004. Inverse spectral decomposition. Expanded Abstr., 74th Ann. Internat. SEG Mtg., Denver: 1786-1789.
- Portniaguine, O. and Castagna, J.P., 2005, Spectral inversion: Lessons from modeling and boonesville case study. Expanded Abstr., 75th Ann. Internat. SEG Mtg., Houston: 1638-1641.
- Press, W.H., Flannery, B.P., Teukolsky, S.A. and Vetterling, W.T., 1992. *Numerical Recipes in C*, 2nd Ed.. Cambridge University Press, Cambridge.
- Puryear, C.I., 2006. Modeling and Application of Spectral Inversion. M.Sc. thesis, University of Houston.
- Robinson, E.A., 1957. Predictive decomposition of seismic traces. *Geophysics*, 22: 767-778.
- Santosa, F. and Symes, W.W., 1986, Linear inversion of band-limited reflection seismograms. *SIAM J. Scientif. Statist. Comput.*, 7: 1307-1330.
- Taylor, H., Banks, S. and McCoy, J., 1979. Deconvolution with the  $l_1$ -norm. *Geophysics*, 44: 39-52.
- Treitel, S. and Robinson, E.A., 1977. Deconvolution-homomorphic or predictive. *IEEE Transact. Geosc. Electron.*, 15: 11-13.